

Error Rate Performance of QPSK-Transmitted Signal for Power Line Communication under Nakagami-like Background Noise

Youngsun Kim, Hui-Myoung Oh, and Sungsoo Choi
 Power Telecommunication Research Center
 Korea Electrotechnology Research Institute (KERI)
 Ansan-city, Gyeonggi-do, Republic of Korea
 Email: yskim, hmoh, sschoi@keri.re.kr;

Abstract—Power line communication is a candidate for communication technology in electric vehicles and home area networks of smart grid. This paper derives the error rate performance of a QPSK-transmitted power line communication system. The Nakagami- m distribution is used as the closed-form background noise model, which was presented by a previous work. We have evaluated the symbol error rate of QPSK systems with both analytical values and computer simulations, and verified its validity through computer simulations.

Keywords-Power Line Communication; Background Noise; Symbol Error Rate; Nakagami- m distribution.

I. INTRODUCTION

Power Line Communication (PLC) has evolved so significantly that it can support various services, ranging from low-speed command and control to high-speed multimedia transmission. There has been commercial deployment of PLC technology, e.g., for Automatic Meter Reading (AMR), in recent years [1]. The performance of AMR using PLC has been analyzed by various researchers (e.g., [2], [3]). PLC is also of great interest due to its possibility as a communication technology for smart grids. The requirements for PLC are presented as an energy management and facility automation systems in smart grids [4]. Furthermore, the possibility of vehicle communications using PLC has been studied. The channel characteristics of an in-vehicle power line were measured and analyzed for PLC [5].

Despite the versatility of PLC, its channel is time-variant and corrupted by unpredictable impulsive noises. Thus extensive research activities on effective channel modeling of background noise, and impulsive noise have been conducted [6], [7]. It was proposed that the amplitude of background noise in power-line channel follows the Nakagami- m distribution [8] [9]. In our previous work, a closed-form expression for the real part of background noise was derived [10]. Using this closed-form expression, we derived the Bit Error Rate (BER) performance of (Binary Phase Shift Keying) BPSK transmission over power line channels and verified its validity by simulations [11].

This paper considers the Symbol Error Rate (SER) of a quadrature-phase shift-keying (QPSK) system. The system model for the QPSK system is presented in Section II. As an

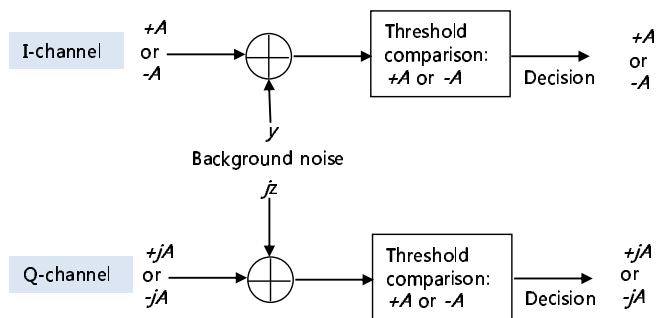


Figure 1. System model for QPSK transmission system

imaginary portion of the background noise is added to the QPSK system, we derive the Probability Density Function (PDF) of the imaginary portion of the background noise in Section III. In Section IV, we analyze the SER of the QPSK-transmitted signal for PLC with Nakagami-like background noise. We verified the accuracy of the analyzed performance by simulations in Section V. The conclusions are presented in Section VI.

II. SYSTEM MODEL

Fig. 1 shows a conventional baseband system model for QPSK transmission. There are in-phase and quadrature channels that are used for the data transmission from the component set, $\{\pm A\}$. As seen in Fig. 1, the QPSK system can be observed as two BPSK systems. Thus, the data recovery is performed in both BPSK systems in a parallel manner. A simple comparison shows the transmitted data has a threshold value 0. Between the transmission and the decision, both channels have background noises, y and z . We consider the background noise only for the ease of analysis. Applying the channel model added by impulsive noise remains as a subject for future work.

As introduced in the previous section, the amplitude spectrum of the background noise of power line can be modeled as a Nakagami- m distribution. Nakagami- m distribution is conventionally used to model a fading channel of wireless communication due to its versatility [12]. From the random

$$f(z) = \frac{1}{\sqrt{\pi}\Gamma(m)} \sqrt{\frac{m}{\Omega}} e^{-\frac{mz^2}{\Omega}} \left\{ \frac{\Gamma(\frac{1}{2}-m)}{\Gamma(1-m)} \left(\frac{mz^2}{\Omega}\right)^{m-\frac{1}{2}} {}_1F_1\left(\frac{1}{2}, \frac{1}{2}+m, \frac{mz^2}{\Omega}\right) + \frac{\Gamma(m-\frac{1}{2})}{\sqrt{\pi}} {}_1F_1\left(1-m, \frac{3}{2}-m, \frac{mz^2}{\Omega}\right) \right\} \quad (11)$$

variable for noise amplitude, α , which follows a Nakagami- m PDF,

$$f(\alpha) = \frac{2m^m \alpha^{2m-1}}{\Gamma(m)\Omega^m} e^{-(m/\Omega)\alpha^2}, \quad \alpha \geq 0 \quad (1)$$

where $\Gamma(\cdot)$ is the Gamma function, m and Ω are parameters defined as $\Omega = E[\alpha^2] = \overline{\alpha^2}$, $E[\beta] = \overline{\beta}$ denoting the expected value of α and $m = \frac{(\overline{\alpha^2})^2}{(\alpha^2 - \overline{\alpha^2})^2} > 0$. Thus Ω is viewed as the power of the amplitude, α . Eq.(1) is close to white Gaussian ($m \approx 1$) at high frequencies (about 25MHz), whereas it becomes a one-sided Gaussian ($m < 1$) at low frequencies (about 5MHz).

The noise amplitude can be divided into real and imaginary parts, y and z , respectively. Then, we apply two components by θ , which is a uniformly distributed random variable from $-\pi$ to π , and we get two random variables as

$$y = \alpha \cos \theta, \quad (2)$$

$$z = \alpha \sin \theta. \quad (3)$$

In a previous work [10], we derived the PDF of the real part of noise, y ,

$$f(y) = \frac{1}{\sqrt{\pi}\Gamma(m)} \sqrt{\frac{m}{\Omega}} e^{-\frac{my^2}{\Omega}} \left\{ \frac{\Gamma(\frac{1}{2}-m)}{\Gamma(1-m)} \left(\frac{my^2}{\Omega}\right)^{m-\frac{1}{2}} \times {}_1F_1\left(\frac{1}{2}, \frac{1}{2}+m, \frac{my^2}{\Omega}\right) + \frac{\Gamma(m-\frac{1}{2})}{\sqrt{\pi}} \times {}_1F_1\left(1-m, \frac{3}{2}-m, \frac{my^2}{\Omega}\right) \right\} \quad (4)$$

for $0 < m < 1$ and $m \neq \frac{1}{2}$. The confluent hypergeometric function of the first kind, ${}_1F_1$, is defined as [13, Chap. 9.2] :

$${}_1F_1(a, b, z) = 1 + \frac{a}{b} \frac{z}{1!} + \frac{a(a+1)}{b(b+1)} \frac{z^2}{2!} + \frac{a(a+1)(a+2)}{b(b+1)(b+2)} \frac{z^3}{3!} \dots \quad (5)$$

We derive the PDF for the imaginary portion of noise, z , in a later section.

III. PDF FOR IMAGINARY PORTION OF NOISE

In this section, we derive the PDF for the imaginary portion of noise, z , in Eq.(3). From Eqs.(1) and (3),

$$\frac{dz}{d\alpha} = \sin \theta, \quad (6)$$

then, a conditional PDF of z subjected to θ , $f(z)|_{\theta}$, can be expressed as

$$\begin{aligned} f(z)|_{\theta} &= \frac{f(\alpha)}{dz/d\alpha} \\ &= \frac{2m^m \alpha^{2m-1}}{\Gamma(m)\Omega^m} e^{-(m/\Omega)\alpha^2} \frac{1}{dz/d\alpha} \\ &= \frac{2m^m \alpha^{2m-1}}{\Gamma(m)\Omega^m \sin^{2m-1} \theta} e^{-(m/\Omega)\frac{z^2}{\sin^2 \theta}} \frac{1}{\sin \theta} \\ &= \frac{2z^{2m-1}}{\Gamma(m)\sin^{2m} \theta} \left(\frac{m}{\Omega}\right)^m e^{-\frac{mz^2}{\Omega \sin^2 \theta}} \end{aligned} \quad (7)$$

using Eqs.(1), (3) and (6). From the fact that the θ is uniformly distributed over $[-\pi, \pi]$, the joint PDF for z and θ , $f(z, \theta)$, is represented as

$$\begin{aligned} f(z, \theta) &= \frac{2z^{2m-1}}{\Gamma(m)\sin^{2m} \theta} \left(\frac{m}{\Omega}\right)^m e^{-\frac{mz^2}{\Omega \sin^2 \theta}} \frac{1}{2\pi} \\ &= \frac{z^{2m-1}}{\pi\Gamma(m)\sin^{2m} \theta} \left(\frac{m}{\Omega}\right)^m e^{-\frac{mz^2}{\Omega \sin^2 \theta}}. \end{aligned} \quad (8)$$

The PDF of the imaginary part of noise, $f(z)$, can be obtained

$$\begin{aligned} f(z) &= \int_{-\pi}^{\pi} f(z, \theta) d\theta \\ &= \int_{-\pi}^{\pi} \frac{z^{2m-1}}{\pi\Gamma(m)\sin^{2m} \theta} \left(\frac{m}{\Omega}\right)^m e^{-\frac{mz^2}{\Omega \sin^2 \theta}} d\theta \\ &= 4 \int_0^{\pi/2} \frac{z^{2m-1}}{\pi\Gamma(m)\sin^{2m} \theta} \left(\frac{m}{\Omega}\right)^m e^{-\frac{mz^2}{\Omega \sin^2 \theta}} d\theta. \end{aligned} \quad (9)$$

Letting $\sin^2 \theta = t$ gives $d\theta = \frac{dt}{2\sqrt{t}\sqrt{1-t}}$, then, Eq. (9) is

$$\begin{aligned} f(z) &= 4 \int_0^1 \frac{z^{2m-1}}{\pi\Gamma(m)t^m} \left(\frac{m}{\Omega}\right)^m e^{-\frac{mz^2}{\Omega t}} \frac{dt}{2\sqrt{t}\sqrt{1-t}} \\ &= \frac{2z^{2m-1}}{\pi\Gamma(m)} \left(\frac{m}{\Omega}\right)^m \int_0^1 t^{-(m+\frac{1}{2})} (1-t)^{-\frac{1}{2}} e^{-\frac{mz^2}{\Omega t}} dt, \end{aligned} \quad (10)$$

which has same integration as that of the real part of noise, $f(y)$, in [10]; thus, we get a closed-form PDF as in Eq.(11) for $0 < m < 1$ and $m \neq \frac{1}{2}$. Then, we can conclude that the amplitude noise of the power line shows the same statistical behavior in both real and imaginary parts of noise.

IV. DERIVATION OF THE ERROR RATE PERFORMANCE

In this section, we derive the error rate performance of the QPSK-modulated signal with noise as described in section II. Fig. 2 shows the signal constellation for the QPSK signal transmission. A transmitter sends the complex symbol, $\pm A \pm$

$$P_1 = \frac{\Gamma(\frac{1}{2} - m)}{2m\sqrt{\pi}\Gamma(m)\Gamma(1 - m)} \left[x^{2m} {}_2F_2 \left(m, m; \frac{1}{2} + m, m + 1; -x^2 \right) \right]_{x=\sqrt{\frac{m}{\Omega}}A}^{\infty} + \frac{\Gamma(m - \frac{1}{2})}{\sqrt{\pi}\Gamma(m)} \left[x {}_2F_2 \left(\frac{1}{2}, \frac{1}{2}; \frac{3}{2} - m, \frac{3}{2}; -x^2 \right) \right]_{x=\sqrt{\frac{m}{\Omega}}A}^{\infty} \quad (17)$$

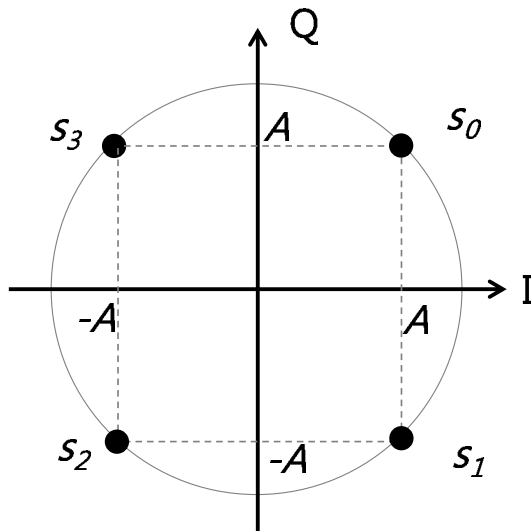


Figure 2. Signal constellation for QPSK

jA , according to the symbol set, $\{s_0, s_1, s_2, s_3\}$ then, the complex decision metric at the receiver, r , is defined as

$$r = \pm A \pm jA + y + jz, \quad (12)$$

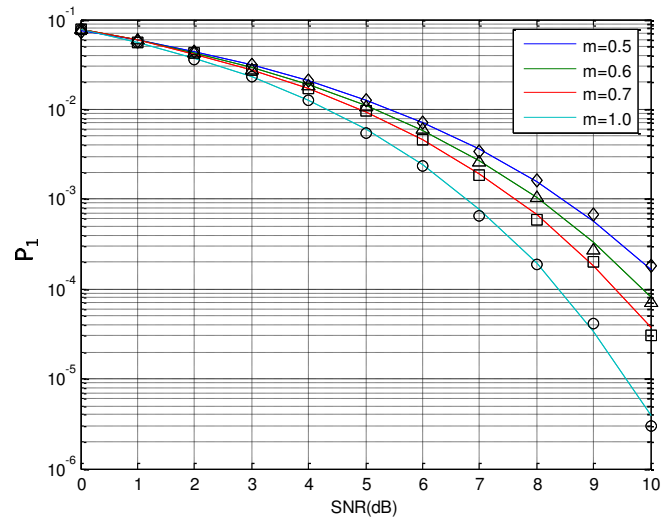
where I and Q channel data, $\pm A \pm jA$, are corrupted by a complex Nakagami background noise, $y + jz$. We assume that four signals are equally probable; thus, the optimal threshold for decision is x and y-axes. For example, if signal s_0 is transmitted and a noise-corrupted received signal falls in the first quadrant, then the decision is correctly made as s_0 ; otherwise, it fails.

When a symbol s_0 is sent, the probability of symbol s_0 is correctly decided, $p(C|s_0)$, and is represented by

$$p(C|s_0) = p(y > 0|s_0) p(z > 0|s_0), \quad (13)$$

which means a noise-corrupted symbol must fall on the first quadrant. We get

$$\begin{aligned} p(y > 0|s_0) &= 1 - \int_{-\infty}^0 p(y|s_0) dy \\ &= 1 - \int_A^{\infty} f(y|s_0) dy \\ &= p(z > 0|s_0). \end{aligned} \quad (14)$$


 Figure 3. Simulated and analyzed evaluations of P_1 with various m values (reprinted from [10])

The probability of s_0 being correctly decided is

$$\begin{aligned} p(C|s_0) &= \left(1 - \int_A^{\infty} f(y|s_0) dy \right)^2 \\ &= 1 - 2 \int_A^{\infty} f(y|s_0) dy + \left(\int_A^{\infty} f(y|s_0) dy \right)^2. \end{aligned} \quad (15)$$

Finally, the symbol error probability, P_e , is given as

$$\begin{aligned} P_e &= 1 - p(C|s_0) \\ &= 2 \int_A^{\infty} f(y|s_0) dy - \left(\int_A^{\infty} f(y|s_0) dy \right)^2 \\ &= 2P_1 - P_1^2, \end{aligned} \quad (16)$$

where we can evaluate the integral part, P_1 , using the result from [11] as Eq.(17). The simulated and the analyzed evaluations of P_1 are depicted in Fig. 3. The X-axis is a dB-scaled Signal-to-Noise Ratio (SNR) value, which is defined as A^2/Ω . For higher values of SNR, P_1^2 becomes very small; then, Eq. (16) can be approximated as

$$P_e \approx 2P_1, \quad (17)$$

which means that the symbol error rate is approximately twice the BER of BPSK. The result is that the SER of QPSK is poorer than that of BPSK in symbol error sense.

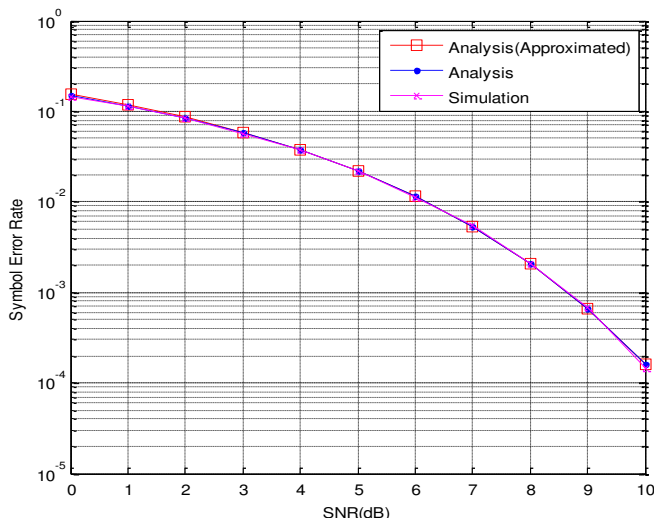


Figure 4. Analyzed and simulated SER performances under Nakagami-like background noise with $m = 0.6$

V. SIMULATION RESULTS

The SER performance of QPSK is simulated with the Monte Carlo method. 10^6 symbols are randomly generated at the transmitter. The generated symbols are corrupted by complex Nakagami-like background noise; then, the demodulated symbols are decided by a threshold comparison as presented in Fig. 1.

Fig. 4 shows the analyzed and the simulated SER performances for $m = 0.6$. The approximated analysis curves obtained from Eq.(17). The simulation results match well with those of the analysis. The accuracy of the approximated analysis is credible for all SNR values. Fig. 5 shows the analyzed and the simulated SER performances for $m = 0.9$. We can observe that a similar accuracy exists between the simulated and the analyzed performances.

VI. CONCLUSION

This paper analyzed and simulated the SER performance of the QPSK-transmitted signal under Nakagami-like background noise. We derived the imaginary portion of the Nakagami-like background noise. The derived result shows that the statistical behavior of the real and the imaginary parts of noise are the same. Next, we derived the SER performance of the QPSK-transmitted signal. For higher values of SNR, the SER performance is approximated to twice the error rate performance of a binary transmitted signal. Simulation was done for randomly generated 10^6 symbols through the Monte Carlo method. The analyzed SER performances agree well with the simulations using various values of m . The BER performance of the QPSK-transmitted signal would be the focus of the future work.

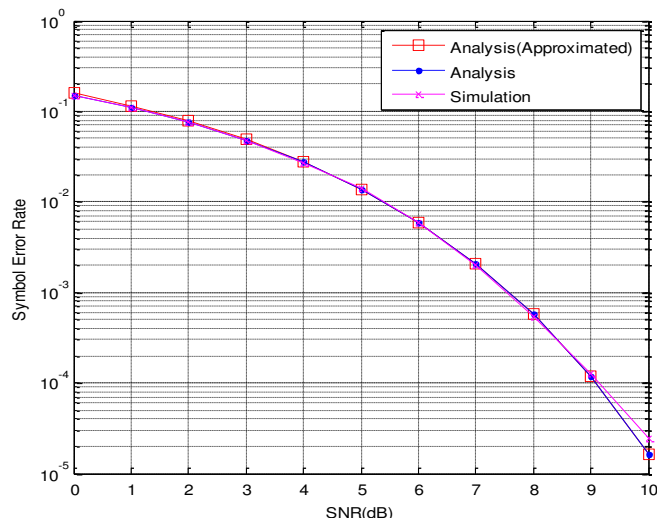


Figure 5. Analyzed and simulated SER performances under Nakagami-like background noise with $m = 0.9$

REFERENCES

- [1] Y. Zhang and S. Cheng, "Power Line Communications," IEEE Potentials, vol. 23, no. 4, pp. 4-8, Oct.-Nov. 2004.
- [2] A. Zaballos, A. Vallejo, M. Majoral and J. M. Selga, "Survey and performance comparison of AMR over PLC standards," IEEE Trans. Power Del., vol. 24, no. 2, pp. 604-613, April 2009.
- [3] B. Sivaneasan, E. Gunawan and P. L. So, "Modeling and performance analysis of automatic meter-reading systems using PLC under impulsive noise interference," IEEE Trans. Power Del., vol. 25, no. 3, pp. 1465-1475, July 2010.
- [4] G. Mumiller, L. Lampe, and H. Hrasnica, "Power line communication networks for large-scale control and automation systems," IEEE Communications Magazines, vol. 48, Issue 4, pp. 106-113, 2010.
- [5] M. Lienard, M. O. Carrion, V. Degardin and P. Degauque, "Modeling and analysis of in-vehicle power line communication channels," IEEE Trans. on Vehicular Technology, vol. 57, Issue 2, pp. 670-679, 2008.
- [6] M. Zimmermann and K. Dostert, "A multipath model for the powerline channel," IEEE Trans. Commun., vol. 50, no. 4, pp. 553-559, April 2002.
- [7] M. Zimmermann and K. Dostert, "Analysis and modeling of impulsive noise in broadband powerline communications," IEEE Trans. Electromagn. Compat., vol. 44, no. 1, pp. 249-258, Feb. 2002.
- [8] M. Nakagami, "The m -distribution - A general formula of intensity distribution of rapid fading," in Statistical Methods in Radio Wave Propagation, pp. 3-36, Pergamon Press, Oxford, U.K, 1960.
- [9] H. Meng, Y. L. Guan and S. Chen, "Modeling and analysis for noise effects on broadband power-line communications," IEEE Trans. Power Del., vol. 20, no. 2, pp. 630-637, April 2005.

- [10] Y. Kim, H-M. Oh and S. Choi, "Closed-form expression of Nakagami-like background noise in power-line channel," IEEE Trans. Power Del., vol. 23, no. 3, pp. 1410-1412, Oct. 2008.
- [11] Y. Kim, Y-H. Kim, H-M. Oh and S. Choi, "BER performance of binary transmitted signal for power line communication under Nakagami-like background noise," Proc. Energy 2011 : The First International Conference on Smart Grids, Green Communications and IT Energy-aware Technologies, pp. 126-129, May. 2011.
- [12] M. K. Simon and M.-S. Alouini, Digital Communications Over Generalized Fading Channels : A Unified Approach to Performance Analysis, New York: Wiley, 2000.
- [13] I. S. Gradshteyn and I. M. Ryzhik, Table of Integrals, Series, and Products, 6th ed., San Diego, CA: Academic, 2000.